# THE FLUORINE EFFECT ON THE GRAIN-GROWTH OF α¹:β¹-SiAlON CERAMICS

## Nurcan ÇALIŞ AÇIKBAŞ [1, *], Hasan MANDAL [2]

[1] Department of Metallurgical and Materials Science Engineering, Bilecik Şeyh Edebali University, Bilecik, Turkey
[2] Sabancı University, Department of Materials Science and Nanoengineering, İstanbul, Turkey

## ABSTRACT

SiAlON ceramics are of major interest for industrial applications due to their excellent mechanical properties. The starting $Si_3N_4$ powder (α or β), the type of sintering additive and sintering conditions govern the microstructural evolution of SiAlON ceramics. In this study, α¹:β¹ SiAlON ceramics with an equal mole intergranular phase content, different type cation systems (Y:Sm:Ca and Ca:Ce) with different molar ratio (30:64:6 and 33:67) were produced by using coarse ($d_{50}$=1 μm) β-$Si_3N_4$ powder. $CaF_2$ and $CaCO_3$ were utilized as Ca sources. Despite the fact that α¹-SiAlON phase cannot be stabilized in Ca:Ce ($CaCO_3$ as a Ca source) system, α¹-SiAlON phase stability and unpredictable α¹-SiAlON grain-growth in both a and c directions was achieved when $CaF_2$ was incorporated in the composition. On the other hand, an increase in α¹-SiAlON amount and more elongated SiAlON grain evolution was observed when $CaF_2$ was used instead of $CaCO_3$ in Y:Sm:Ca cation system. Furthermore, using $CaF_2$ instead of $CaCO_3$ gave rise to an increase in densities. Therefore, the substantial effect of $CaF_2$ on abnormal grain growth and α¹-SiAlON phase stabilization was observed.

**Keywords:** Fluorine, Grain growth, α¹-SiAlON stability, Microstructure

## 1. INTRODUCTION

Microstructure evolution of silicon nitride based ceramics is controlled by properties of initial $Si_3N_4$ powder, sintering additives and sintering conditions. Composition and particle size of starting $Si_3N_4$ powder have been known to have a significant effect on microstructure development. Generally two forms of silicon nitride powders: α-$Si_3N_4$ and β-$Si_3N_4$ are used as a starting powder. Wild and co-workers [1] have shown that a small amount of oxygen is incorporated into the atomic structure of the α phase; the approximate formula is $Si_{11.5}N_{15}O_{0.5}$, whereas the β-phase is pure β-$Si_3N_4$. Thus α-$Si_3N_4$ powder is used more common due to higher reactivity than β-$Si_3N_4$ powder. It is well known that α phase is low temperature configuration of $Si_3N_4$ and transform to β-phase at ~1410ºC< [2]. Other reason for the preference of α-$Si_3N_4$ powder is elongated β grain formation after α→β phase transformation [3]. However, fine α-$Si_3N_4$ powders are expensive and this is a key problem for large scale applications. When β-$Si_3N_4$ powder is used as a starting powder, elongated grain formation and densification are rather difficult due to aforementioned reasons [4]. On the other hand, β-$Si_3N_4$ powders can be produced in an economic route with combustion synthesis [5]. Use of such powders may open up possibilities for wider applications of SiAlON ceramics.

The second parameter on microstructure evolution is type of sintering additives. Most of the investigations had been focused on the influence of sintering additives on grain growth [6,7]. The understanding of grain growth kinetics is a key issue in order to design high toughness and high strength materials. It is generally accepted that grain growth anisotropy increase with increasing cation size due to preferred segregation of large cations on the prism plane of grains [8,9]. Besides, sintering additives have an effect on intergranular phase chemistry [10]. In SiAlON ceramics, the influence of cations on the interfacial properties is rather different than $Si_3N_4$ ceramics since some $Al^{3+}$ cations enter into the crystal structure or/and remain in the intergranular phase. The third important parameter is sintering

*Corresponding Author: nurcan.acikbas@bilecik.edu.tr

condition. Today silicon nitride ceramics are densified by presureless sintering, gas pressure sintering, hot pressing or hot isostatic pressing. Gas pressure sintering of $Si_3N_4$ ceramics at higher temperatures (>1800ºC) develops an in situ composite microstructures with a high fracture toughness [11].

There exist some studies on microstructural evolution of SiAlON ceramics when use of $\beta$-$Si_3N_4$ as a starting powder [12-14]. However there is no study on the effect of $CaF_2$ sintering additive on microstructural evolution of SiAlON ceramics. In this respect this study is novel. Therefore the aim of this study is to evaluate the effect of fluorine on SiAlON grain growth as well as to correlate this $\alpha^1$-SiAlON phase stability and sample density.

## 2. MATERIALS AND METHOD

The starting $\beta$-$Si_3N_4$ powder (Beijing Chanlian-Dacheng Trade Co., Ltd., China) was produced by combustion synthesis and consisted 100% $\beta$-$Si_3N_4$ phase. Table 1 provides the specification of as-received and milled $\beta$-$Si_3N_4$ powder, which contains 3 wt.% oxygen. Primary particle size of $\beta$-$Si_3N_4$ powder was measured to be around 10 µm by laser diffraction method (Figure 1). Attrition milling in water was performed to decrease the average particle size of $\beta$-$Si_3N_4$ starting powder to 1 µm. The corresponding starting powder was designated as B1. The particle size distribution graph of B1 powder was given in Figure 2. Representative SEM images of as-received and milled $\beta$-$Si_3N_4$ powders and XRD analysis of starting $\beta$-$Si_3N_4$ powders are shown in Figure 3 and 4, respectively. Starting powder contains Fe, $Fe_2Si$, $FeSi_2$ and Si as a major impurity.

**Table 1.** Specifications of $\beta$-$Si_3N_4$ powders

| Starting Powders | B (as-received) | B1 |
|---|---|---|
| $\alpha$:$\beta$ Phase Ratio | 100$\beta$ | 100$\beta$ |
| $d_{50}$ (µm) | 10 | 1.2 |
| $d_{90}$ (µm) | 36 | 2.4 |
| $d_{10}$ (µm) | 2.4 | 0.5 |
| Milling time (hr) | - | 9 |
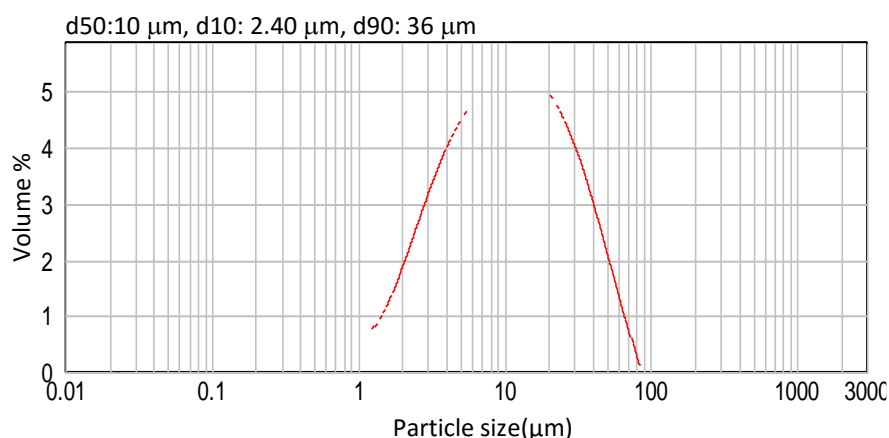


**Figure 1.** Particle size distribution graph of as-received $\beta$-$Si_3N_4$ powder
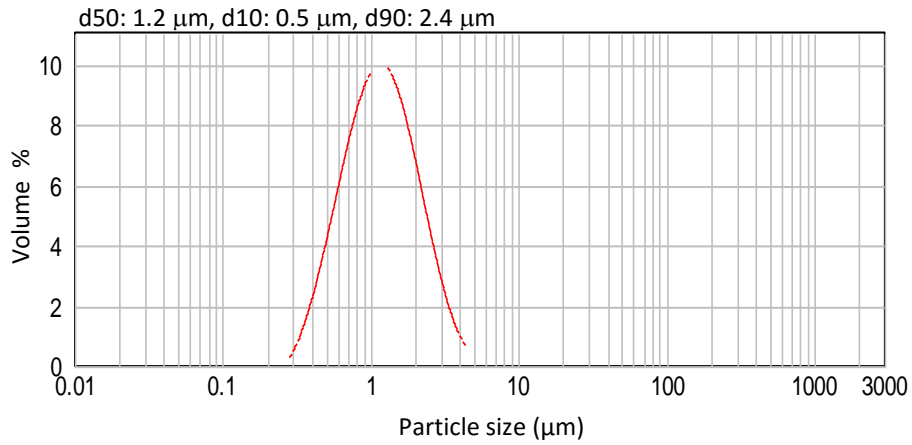
d50: 1.2 μm, d10: 0.5 μm, d90: 2.4 μm



**Figure 2.** Particle size distribution graph of B1 powder
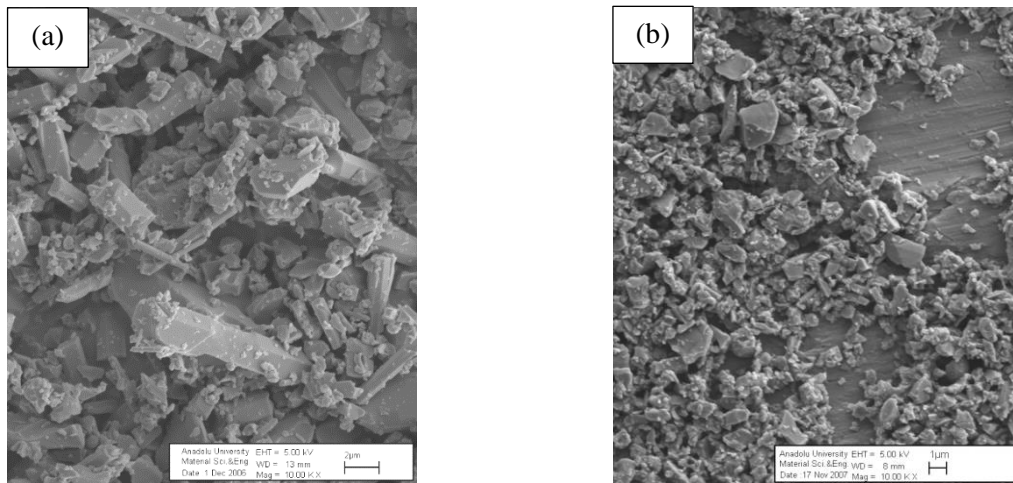


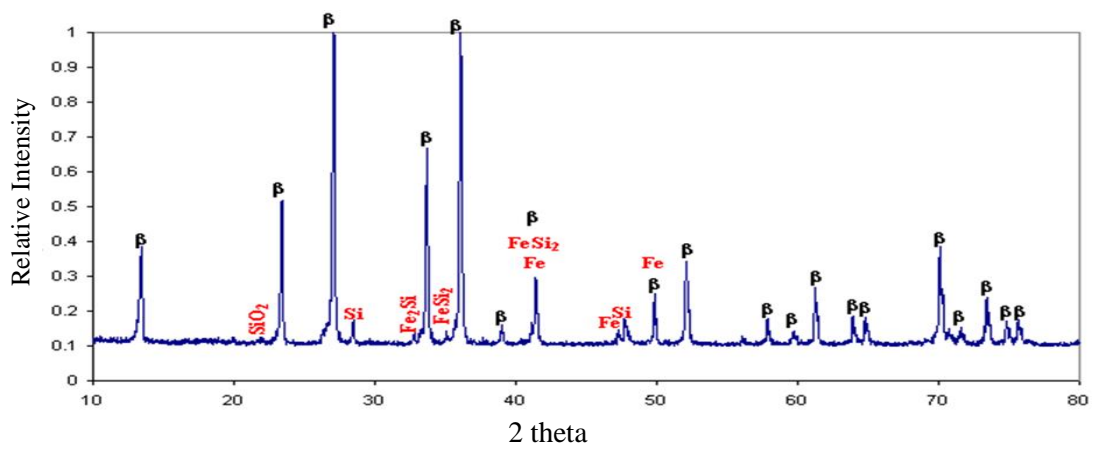**Figure 3.** SE-SEM images of (a) as-received $\beta$-$Si_3N_4$ powder (b) B1powder



**Figure 4.** XRD spectra of as-received $\beta$-$Si_3N_4$ powder ($\beta$: $\beta$-$Si_3N_4$)

$30\alpha^1{:}70\beta^1$ SiAlON composition was designed where hardness of $\alpha^1$-SiAlON and toughness of $\beta^1$-SiAlON wanted to be utilized. Y:Sm:Ca and Ca:Ce multi cation systems with different molar ratio (30:64:6 and 33:67) were chosen. High purity AlN powder (H Type, Tokuyama Corp. Japan) containing 1.6 wt% O, $Al_2O_3$ (Alcoa A16-SG, Pittsburgh, USA), $Y_2O_3$ (>99.99%, Treibacher, Austria), $Sm_2O_3$ (>99.9%, Stanford Materials Corp., USA), $CeO_2$ (>99.99%, Aldrich, Germany), $CaCO_3$ (>99.75%, Reidel-de Haen, Germany) and $CaF_2$ (>99.99%, Aldrich, Germany) were used as sintering additives. Y-Sm- Ca and Ca-Ce multi cation doping systems were chosen with the aim to produce self reinforcement microstructures. CaO was used to avoid $\alpha^1$ to $\beta^1$-SiAlON transformation, $Y_2O_3$ and/or $Re_2O_3$ (where ZRe>62)) to increase the stability and hardness of $\alpha^1$-SiAlON and $Sm_2O_3/CeO_2$ (where ZRe<62) to develop elongated $\beta^1$-SiAlON grains to increase fracture toughness.

The formulated composition contains high enough liquid phase (0.033 moles) to provide easy densification. Theoretical liquid phase content was calculated take into account the amount of sintering additives in the composition. However, to prevent the side effect of intergranular phase, refractory melilite ($Ln_2Si_{3-x}Al_xO_{3+x}N_{4-x}$) phase crystallization was aimed. Designed SiAlON compositions were prepared by plenatory milling for 90 min at 300 rpm in isopropyl alcohol using $Si_3N_4$ balls. The slurries were then dried in a rotary evaporator and sieved through 75 μm. The powders were uniaxially pressed at 25 MPa, 15mm $\phi$ and 4 mm in thicknesses and subsequently cold isostatically pressed at 300 MPa to improve green density. The pellets were sintered using a two-step gas pressure sintering cycle. In the case of one step sintering, gas remains in the pores and effect the densification negatively. Therefore in the first step must be reached to closed pores level at certain nitrogen pressure to prevent $Si_3N_4$ decomposition and then should go up to high pressures to promote the densification. The first step is called as pre-sintering and was carried out at 1900°C for 60 min, 0.5 MPa nitrogen gas pressure and second step at 1940 °C for 120 min of 2.2 MPa nitrogen gas pressure and then the furnace was allowed to cool at a rate of 5°C/min.

Archimedes principle was used to measure the bulk density of samples after sintering. Theoritical density of samples was found by He gas picnometer. %T.D. values were calculated with following equation.

% Theoritical Density= (Bulk density / Theoritical density) * 100          (1)

The types of crystalline phases and the $\alpha^1{:}\beta^1$-SiAlON phase ratios were determined by means of X-ray diffraction analyses (XRD-Rigaku, Cu-Kα radiation). The $\alpha^1{:}\beta^1$-SiAlON phase ratios were found by quantitative estimation from the XRD patterns using the integrated intensities of the (102) and (210) reflections of $\alpha^1$-SiAlON and the (101) and (210) reflections of $\beta^1$-SiAlON by the following equation:

$$\frac{I_\beta}{I_\beta + I_\alpha} = \frac{1}{1 + K\left[\left(1/w_\beta\right) - 1\right]}$$          (2)

where $I_\alpha$ and $I_\beta$ are observed intensities of $\alpha^1$ and $\beta^1$-SiAlON peaks, respectively, $w_\beta$ is the relative weight fraction of $\beta^1$-SiAlON, and K is the combined proportionality constant resulting from the constants in the two equations, namely:

$I_\beta = K_\beta * W_\beta$          (3)
$I_\alpha = K_\alpha * W_\alpha$          (4)

which is (0.518 for $\beta$ (101) – $\alpha$ (102) reflections and 0.544 for $\beta$ (210) – $\alpha$ (210) reflections [17]. The lattice parameters of SiAlONs were measured with silicon powders as the internal standard. Lattice parameters are calculated according to following formula, where d is the distance between the planes, a and c are lattice parameters. Calculation was done by using (101) and (210) planes.

$$\frac{1}{d^2} = \frac{4}{3}\left(\frac{h^2 + hk + k^2}{a^2}\right) + \frac{l^2}{c^2} \tag{5}$$

The samples were prepared before SEM examination. Cold moulded specimens were subjected to grinding and polishing processes. Grinding of sample was carried out with abbresive papers with grid size of 200, 400, 600, 800 and 1000 respectively. Subsequently, polishing of sample was made by tetrapol device by using DAC and NAP clothes with its unique suspension. Time for DAC 5 min and for NAP 3 min. After each step the surfaces of the samples were treated with metylalcohol and dried with air blowing. Polished surfaces of the sintered samples were gold coated prior to examination in a Zeiss VP50-Supra type scanning electron microscope (SEM) by using back-scattered electron imaging mode.

## 3. RESULTS AND DISCUSSION

The results of phase analysis, bulk density, and theoretical density and weight losses are given in Table 2. >%99.75 theoretical density was achieved in all compositions. Considerably high (≥%2.19) weight loses was observed due to impurities in initial $\beta$-$Si_3N_4$ powder. By using $CaF_2$ instead of CaO, bulk densities increased %0.6-0.7 and weight loses %34-60. F in structure is evaporated as a $SiF_4$ and hence this phenomena lead to more weight loses [18,19].

In Ca:Ce cation sytem, $\alpha^\iota$-SiAlON phase stability was not achieved (100 $\beta^\iota$-SiAlON) employing CaO in Ca:Ce containing composition. Use of $CaF_2$ instead of CaO resulted in 81$\beta^\iota$:19$\alpha^\iota$-SiAlON phase composition. Designed phase ratios (70$\beta^\iota$:30$\alpha^\iota$) was not achieved in both cases (Figure 5). Clarke stated that [20] if initial $Si_3N_4$ powder include Cl/F as a impurity, $\alpha \rightarrow \beta$-$Si_3N_4$ phase transformation retarded considerably. Chlorine remains structure as a silisiumchlorid form until 1750°C and so stabilize $\alpha$-$Si_3N_4$ phase.

There are three approaches why $\alpha^\iota$-SiAlON phase stability was achieved in the case of employing $CaF_2$ instead of CaO. The first one is decrease in oxygen content in intergranular phase may result in $\alpha^\iota$-SiAlON phase stability [21]. $\alpha^\iota \leftrightarrow \beta^\iota$-SiAlON phase transformation depends on starting composition, type of sintering additives, viscosity of liquid phase and liquid phase content [22]. Excess oxygen in the liquid phase causes a decrease in the viscosity of the liquid phase and hence provides $\alpha^\iota \leftrightarrow \beta^\iota$-SiAlON phase transformation. Previously $\alpha^\iota \rightarrow \beta^\iota$-SiAlON phase transformation was observed in Ca-$\alpha^\iota$-SiAlON and Y-$\alpha^\iota$-SiAlON systems [23].

$\alpha^\iota$-SiAlON + Oxide $\rightarrow \beta^\iota$-SiAlON
$\beta^\iota$-SiAlON + Nitride$\rightarrow \alpha^\iota$-SiAlON

chemical reactions may progress depending on liquid phase composition. Besides, $\alpha^\iota \rightarrow \beta^\iota$-SiAlON phase transformation between 1300-1600°C occurred during slow cooling rates [24]. In this study, a slow cooling regime with 5°C/min. was applied. Therefore $\alpha^\iota \rightarrow \beta^\iota$-SiAlON phase transformation is possible.

**Table 2.** Densification and phase analysis results of SiAlON samples (%T.D.: percent theoretical density, %W.L: percent weight loses, IGP: Intergranular phase)

| Cation system | Sintering Additives | Bulk Density (gr/cm³) | %T.D. | %W.L. | β¹:α¹ Ratio | IGP Chemistry | Lattice Parameters |
|---|---|---|---|---|---|---|---|
| Y:Sm:Ca (30:64:6) | $Y_2O_3$ $Sm_2O_3$ CaO | 3.3518 | 99.90 | 2.19 | 73β¹:27α¹ | Melilite | a: 7.6192±0.0022 c: 5.7082±0.0023 |
| Y:Sm:Ca (30:64:6) | $Y_2O_3$ $Sm_2O_3$ $CaF_2$ | 3.3715 | 99.99 | **2.94** | 68β¹:32α¹ | Melilite | a: 7.6192±0.0012 c: 5.7082±0.0014 |
| Ca:Ce (33:67) | CaO $CeO_2$ | 3.2369 | 99.75 | 3.33 | **100β¹** | **Amorphous** | a: 7.6210±0.0015 c: 5.7027±0.0018 |
| Ca:Ce (33:67) | $CaF_2$ $CeO_2$ | 3.2593 | 99.99 | **5.30** | 81β¹:19α¹ | **Amorphous** | a: 7.6210±0.0021 c: 5.7027±0.0022 |
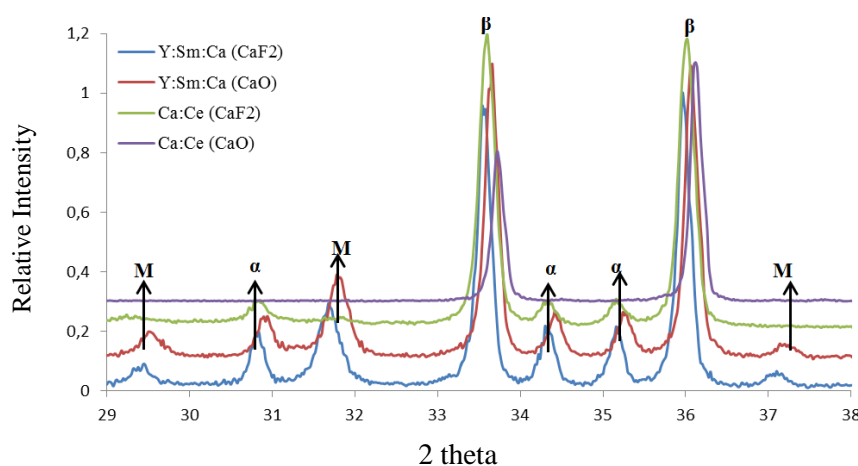


**Figure 5.** XRD graph of SiAlON samples (α: α¹-SiAlON, β: β¹-SiAlON, M: Melilite phase)

The second approach is $CaF_2$ addition may cause more Ca substitution in α¹-SiAlON crystal structure as evidenced by the increase in the density of samples from 3.2369 to 3.2593 gr/cm³. Since no pores were observed in microstructural observations, this is an evidence of entering more Ca in the case of $CaF_2$ addition.

The third and last approach is, $CaF_2$ may provide more α¹-SiAlON phase seeding since its melting temperature is lower as compared to CaO (1423°C for $CaF_2$ and 2572°C for CaO) and so it lowers eutectic temperature and viscosity in oxynitride liquid phase. Although Ce cation is known as a nitrogen rich melilite phase stabilizer, melilite phase crystallization was not achieved whether $CaF_2$ or CaO was used in equimolar Ca and Ce.

Since Y:Sm:Ca dopant system include less CaO/$CaF_2$ content compared to Ca:Ce system, ~%20 increase (27α→33α) in α¹-SiAlON phase amount was observed when using $CaF_2$ instead of CaO. Melilite phase crystallization was provided in both materials (including CaO/$CaF_2$), due to high Sm content (64%). Increase in α¹-SiAlON phase content may be resulted from substitution of more Ca in the case of using $CaF_2$ powder. In order to prove this phenomenon a and c crystal parameters were calculated. However it was observed that a and c parameters were similar.

SEM images CaO or $CaF_2$ used Y:Sm:Ca doped SiAlON samples were given in Figure 6. The microstructure of the samples revealed the presence of three different contrasting phases. The prismatic grains with darker contrast were β¹-SiAlON, the equiaxed grains with grey contrast were α¹-SiAlON and small white areas were intergranular phase due to the strong electron-scattering characteristic of

the heavy metals. Increase in $\alpha^1$-SiAlON content was observed with addition of $CaF_2$. $\beta^1$-SiAlON grains turned into more elongated morphology when $CaF_2$ was used instead of CaO contrary to $\alpha^1$-SiAlON grains was getting more equiaxed shape.

Regarding Ca:Ce doped SiAlON composition, despite the fact that $\alpha^1$-SiAlON phase cannot be stabilized in Ca:Ce ($CaCO_3$ as a Ca source) system, $\alpha^1$-SiAlON phase stability and unpredictable $\alpha^1$-SiAlON grain-growth in both a and c directions was easily achieved (Figure7). The grain growth mechanism of $\alpha^1$-SiAlON is related to liquid phase content and viscosity. In this case addition of $CaF_2$ may lead to decrease in viscosity of liquid phase and provide effective mobility of atoms in liquid phase. $CaF_2$ addition didn't provide abnormal grain growth in Y:Sm:Ca doped SiAlON. This case may be resulted from the difference in viscosity of liquid phase, in both (Ca:Ce and Y:Sm:Ca) cation system.
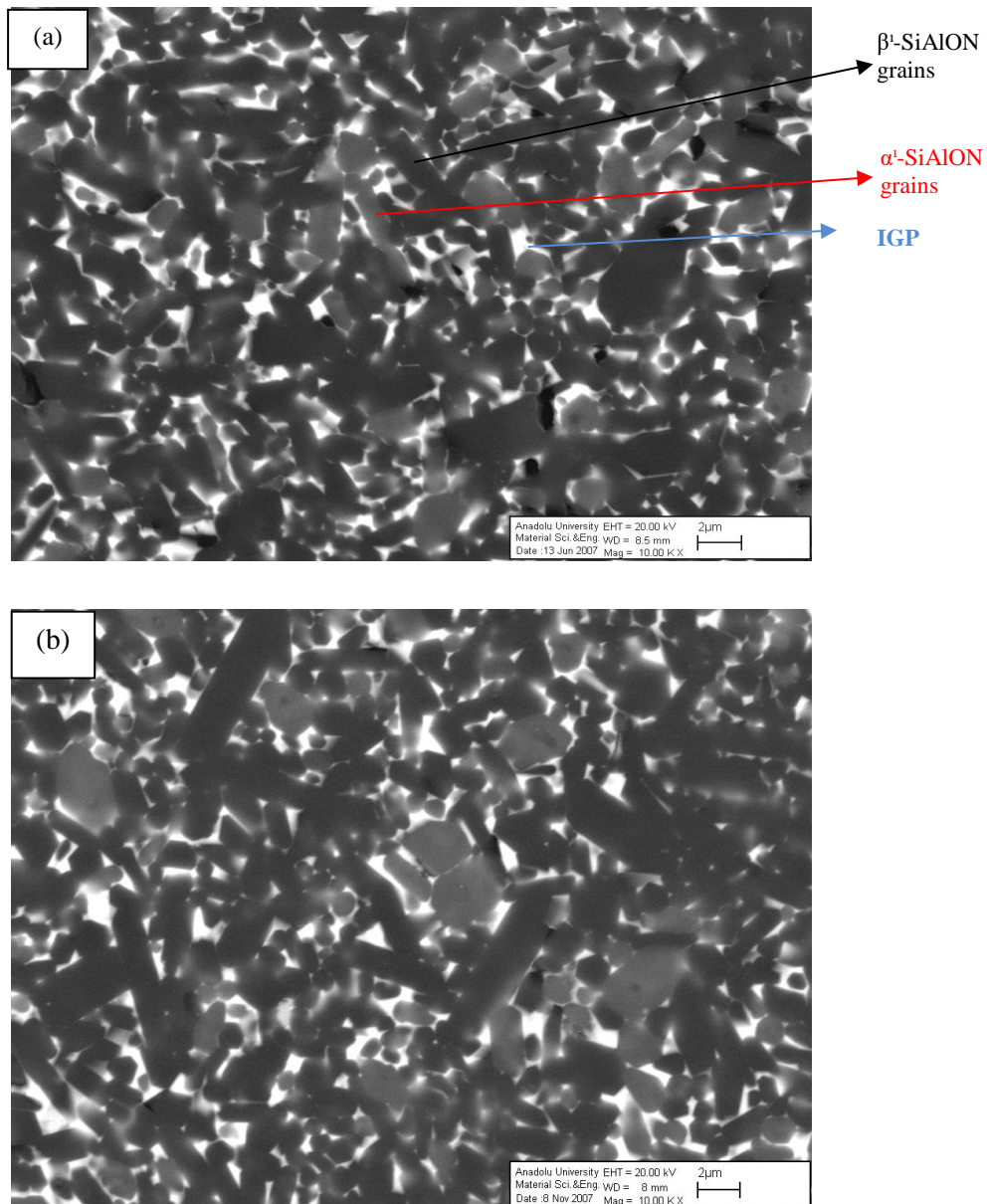


**Figure 6.** Representative BSE-SEM images of Y:Sm:Ca doped SiAlON with **(a)** CaO and **(b)** $CaF_2$ as a Ca source
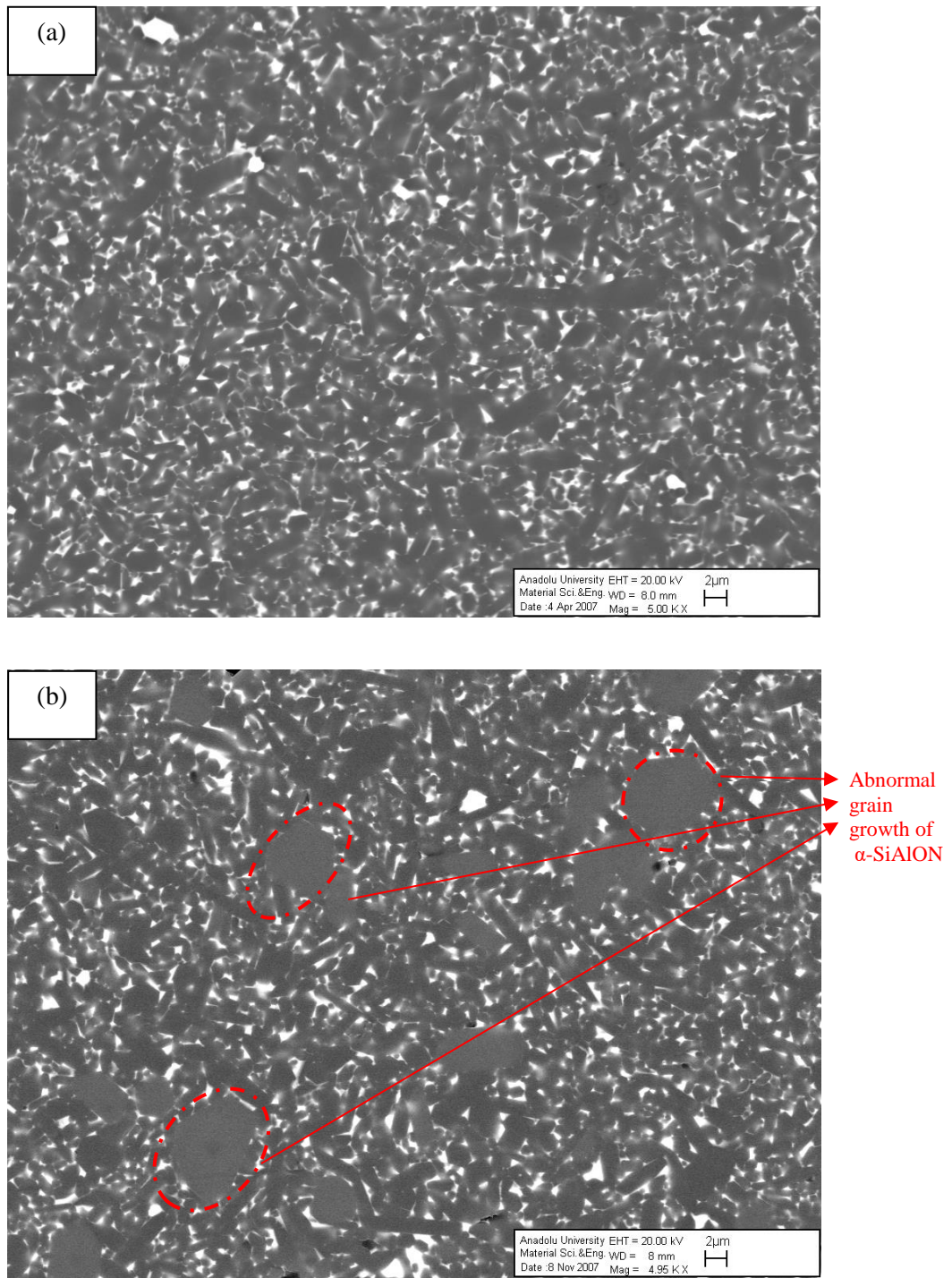
**Figure 7.** Representative BSE-SEM images of Ca:Ce doped SiAlON with **(a)** CaO and **(b)** CaF$_2$ as a Ca source

## 4. CONCLUSIONS

This study contains results of original research work on the effect of $CaF_2$ on $\alpha^!$-SiAlON phase stability, abnormal grain-growth, intergranular phase chemistry and density in $\alpha^!$:$\beta^!$-SiAlON ceramics. Based on the experimental results and observations, the following conclusions were drawn:

1. Despite the fact that $\alpha^!$-SiAlON phase cannot be stabilized in Ca:Ce ($CaCO_3$ as a Ca source) system, $\alpha^!$-SiAlON phase stability and unpredictable $\alpha^!$-SiAlON grain-growth in both a and c directions was easily achieved when $CaF_2$ was incorporated in the composition. On the other hand, an increase in $\alpha^!$-SiAlON amount and more elongated SiAlON grain evolution was observed when $CaF_2$ was used instead of $CaCO_3$ in Y:Sm:Ca cation system.

2. The use of $CaF_2$ instead of $CaCO_3$ gives rise to an increase in densities in both cation systems.

3. Although Ce cation is known as a nitrogen rich melilite phase stabilizer, melilite phase crystallization was not achieved whether $CaF_2$ or CaO was used in equimolar Ca and Ce.

## REFERENCES

[1] Wild S, Grieveson P, and Jack KH. Special Ceramics. In: Popper P, editor. The British Ceramic Research Association, 1972, p. 385-395

[2] Mandal H, Thompson DP, Ekström T. Reversible $\alpha \rightarrow \beta$-SiAlON transformation in heat-treated sialon ceramics, J. Eur. Ceram. Soc., 12: 421-429, 1993.

[3] Lee DD, Kang SJL, Petzow G, Koon DK. Effect of $\alpha$ to $\beta$ phase transition on the sintering of silicon nitride ceramics. J Am Ceram Soc.73, p.767–769, 1990.

[4] Hirosaki N, Akimune Y, Mitomo M. Quantitative Analysis of Microstructure of Silicon Nitride Ceramics. J. *Ceram. Soc.* Japan, p. 1239, 1993.

[5] Lee W-C, Chunga S-L, Combustion synthesis of Si3N4 powder. J. Mater. Research.12 :03. p.805-811, 1997.

[6] Satet RL, Hoffmann MJ. Grain growth anisotropy of beta silicon nitride in rare earth doped oxynitride glasses. J. Euro. Ceram. Soc. 24. P. 3437-3445, 2004.

[7] Mitomo M, Tsutsumi M, Tanaka H, Uenosono S, Saito F. Grain Growth During Gas Pressure Sintering of $\beta$-Si$_3$N$_4$. J. Am. Ceram. Soc., 73, p.2441-45, 1990.

[8] Shibata N, Pennycook SJ, Gosnell TR, Painter SG, Shelton WA, Becher PF. Observation of rare earth segragation in silicon nitride ceramics at subnanometre dimensions. Nature, 428, p.730-33, 2004.

[9] Satet RL, Hoffmann MJ, Influence of the rare-earth element on the mechanical properties of RE–Mg-bearing silicon nitride, Jour. Amer. Ceram. Soc.88:9, p. 2485-2490, 2005.

[10] Acikbas Calis N, Kara A, Turan S, Kara F, Mandal H, Bitterlich B. Influence of type of cations on intergranular phase crystallization of SiAlON ceramics. Mater. Sci. Forum. 554, p.119–122, 2007.

[11] Mitomo M, Tsutsumi M, Tanaka H, Uenosono S, Saito F. Grain Growth During Gas Pressure Sintering of $\beta$-Si$_3$N$_4$. J. Am. Ceram. Soc., 73, p.2441-45, 1990.

[12] Ekström T, Ingelström N, Brage R, Hatcher M, Johansson T. α-β-SiAlON ceramics made from different silicon nitride powders. J. Am. Ceram. Soc. 71, p.1164-1170, 1988.

[13] Li YW, Wang P L, Chen WW, Cheng YB, Yan DS. Phase formation ve microstructural evolution of Ca α-SiAlON using different $Si_3N_4$ starting powders. J. Euro. Ceram. Soc., 20, p.1803-1808, 2000.

[14] Rosenflanz A. α-SiAlON: phase stability, phase transformations, and microstructural evolutions. PhD thesis. Michigan University; 1997, p.178–9.

[15] Mandal H, Kara F, Turan S, Kara A. Multication doped α:β-SiAlON ceramics, US Patent, 2004/0067838A1.

[16] Calis Acikbas N, Yurdakul H, Mandal H, Kara F, Turan S, Kara A, Bitterlich B. Effect of sintering conditions and heat treatment on the properties, microstructure and machining performance of α:β-SiAlON ceramics. J. Euro. Ceram. Soc.,p. 1321–1327, 2012.

[17] K. Liddell, X-ray analysis of nitrogen ceramic phases. MSc thesis, University of Newcastle upon Tyne, UK, 1979.

[18] Hanifi AR, Genson A, Pomeroy, MJ, Hampshire S. An introduction to the glass formation and properties of Ca-Si-Al-O-F glasses. Mater. Sci. Forum, 554, p.17-23, 2007.

[19] Genson A, Hanifi AR, Put AV, Pomeroy M J, Hampshire S. Effect of fluorine and nitrogen anions on properties of Ca-Si-Al-O glasses. Mater. Sci. Forum, 554, p.31-35, 2007.

[20] Clarke DR. Densification of silicon nitride: effect of chlorine impurities. J. Am. Ceram. Soc., 1, p.21-23, 1982.

[21] Acikbas Calis N, Demir O. The effect of cation type, intergranular phase amount and cation mole ratios on z value and intergranular phase crystallisation of SiAlON ceramics. Ceram. Int. 39, p.3249-3259, 2013.

[22] Mandal H, Thompson DP. Reversible α→β phase transformation in heat treated SiAlON Ceramics. J. Euro. Ceram. Soc., 12, p.421-429, 1993.

[23] Hampshire S, Park HK, Thompson DP, Jack KH. α-SiAlON ceramics, *Nature,* 274, p.880, 1978.

[24] Mandal H, Oberacker R, Hoffmann MJ, Thompson DP. α-SiAlON Ceramics Densified with Mixed Oxide Sintering Additives. Mater. Sci. Forum, 325, p.207-212, 20